KSME Journal, Vol. 9, No. 3, pp. 323~335, 1995

Design of Magnetically Suspended Frictionless Manipulator

Kyihwan Park*, Kee-Bong Choi*, Soo-Hyun Kim* and Yoon Keun Kwak*

(Received Desember 17, 1994)

Magnetically suspended frictionless manipulator is designed to improve the resolution and position accuracy. In order to increase the dynamic stability, the magnetically suspended manipulator is constructed using push-and-push forces. Using the force analysis, the design and modeling processes of the manipulator are achieved. The proposed modeling process is experimentally verified from free vibration of the manipulator. Comparison is made between the natural frequencies from the modeled dynamic equation and those from experimentally obtained.

Key Words: Micro-Machine, Magnetic Suspension System, Push-and-Push Force, Antagonistic Structure, Eulerian Angles

1. Introduction

Ideally, automation of small scale process will involve small scale equipment capable of high precision and speed. The required accuracy and repeatability will be dictated by the size of features on each application. Since these features are currently about a micron in size, we refer to machines capable of this level of precision as micro-machine and to the entire automation process as micro-automation. Micro-automation poses significantly different problems from automation on a large scale. In particular, large scale automation systems typically deal with sizable friction whereas micro-automation system must minimize friction in order to obtain submicron precision and to avoid particulate generation. Further, the typical goals in the large scale automation are an ability to handle high payloads, and apply large forces, whereas in micro-automation one is more likely to be interested in the ability to deliver well controlled, delicate forces, and to transport small payloads. These inherent differences between them suggest that the methods appropriate for one may not be appropriate for the other.

In this paper, as one of eletromagnetic approaches, we are examining the micro positioning technology capable of providing high precision and speed using a magnetic levitation(suspension) manipulator, which has noncontact physical forces between the manipulator and base to separate them. The major advantages of levitation are that friction can be removed, and that the manipulator can operate as a rigid body rather than using jointed parts, which means that position errors do not compound, the dynamic behavior is simple to model. The major disadvantage of levitation on small scales is that the levitation system is inherently unstable, and hence control can be computationally intensive.

The development of magnetic suspended micro-machines has been reported in Tsuda et. al., Hollis et. al., and Ohnuki et. al.. Tsuda et. al. (Tsuda, 1987) have designed a magnetically supported intelligent hand (MSIH) which uses active DC-type magnetic bearings. Feedforward and PD control schemes are used to control position and altitude. Using precise control, the mechanism can carry out various automatic assembly tasks like an active/advanced remote center compliance(RCC) device. Hollis et. al. (Hollis, 1987) have designed a hexagonal shaped

* Department of Mechanical Engineering, Korea Advanced Institute of Science and Technology(KAIST), 373-1, Kusong-dong, Yusong-gu, Taejon 305-701, Korea

magnetic suspended wrist using permanent magnets and air-core electromagnets. For this wrist, a quite different moving-coil manipulator was chosen comparing to conventional magnetic bearing manipulator with magnetic gaps wide enough to allow 6 degree-of-freedom motion. A digital PID control loop was implemented with lateral effect sensor on the one-dimensional test setup used for force characterization due to complexity of control for multi degree-of-freedom. Ohnuki et. al. (Ohnuki, 1982) also built micro-machine using a combination of magnetic drive and spring suspension. In their prototype, which has been used for motion of an optical disk head, rubber strands connect the rotor and the stator. However, this system can not be called as a pure magnetic suspension system because a physical spring suspension is used.

Since magnetic levitation(suspension) system is inherently unstable, most concern is focused on a magnetic circuit design so as to increase the system stability. The unstable features in the magnetic suspended micro-machine pose a large control effort. If more stable degree-of-freedom is assured, the control effort is much reduced. Hence, the design of the magnetic suspended positioning system to be proposed in this paper is focused on how to utilize efficiently the force characteristics in order to increase the system dynamic stability. For this, the magnetic suspension system with robust 6 degree-of-freedom motion using push-and-push forces is proposed to maintain in-plane and out-of-plane motion stability of the manipulator. It is capable of $1\sim2$ mm translational movement and $1\sim2°$ rotational movement. The antagonistic structure using push-and-push forces permits a simple design and robust stability as well as high accuracy and speed. Further, a moving-magnet type configuration adopted for easy realization of the antagonistic structure gives many advantages in design and control aspects. In this work, design and modeling of the magnetic suspension system are introduced. Henceforth, we call a magnetic levitation(suspension) system as a maglev system for short.

We have aimed to use the maglev positioning system for semiconductor devices such as a bond quality tester or analytical probe since it can satisfy the essential demand of semiconductor fabrication : dust free environment as well as high accuracy. Though some applications require only three translational motions, we will develop a maglev positioning system which is also capable of rotational motions with the consideration of expanding its application.

2. Force Analysis of a Solenoid/ Permanent Magnet

A magnetic suspension system uses two magnetic components, one of which must be active if motion control is to be accomplished(Sinha, 1987). We have chosen in our work to use rare earth passive magnets mounted on the micro-positioner and air core solenoid electromagnets fixed on the base frame. This particular combination, named as a moving-magnet type manipulator, permits the micro-positioner to work without a power or signal tether to the moving manipulator, improves the positioning accuracy due to the freedom from temperature expansion of the positioner, and uses a drive system which is very linear and thus predictable in behavior.

Air-core solenoid has a few advantages over an iron core in that it has no hysteresis, no eddy current loss, and no saturation of flux density. These characteristics all serve to increase the accuracy which can be achieved. Permanent magnet is being used in many applications of small magnetic systems because it can supply a sufficient force and it is suitable for compact design. Hence for the design of maglev system, one would prefer using an air core solenoid and permanent magnet in pair.

For a current element which is one portion of the current distribution as shown in Fig. 1, the magnetic field $d\boldsymbol{B}$ at the point of concern, P is given in vector form as(Hayt, 1989)

$$d\boldsymbol{B}=\frac{\mu_o i}{4\pi}\left(\frac{d\boldsymbol{S}\times\boldsymbol{r}}{r^3}\right), \tag{1}$$

where i is a flowing current, and $d\boldsymbol{S}$ is the current element length and its direction is tangent to the

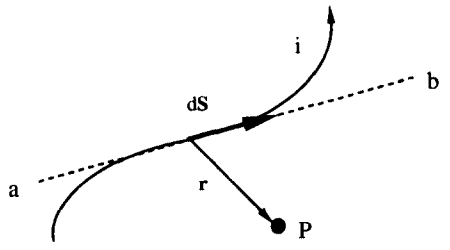

Fig. 1 Current element

conductor(dashed line a-b). μ_o is a permeability of the free space given as $4\pi\times10^{-7}$, and r is a distance from the current element to the point P. The resultant field at P is found by integrating(1), or

$$\boldsymbol{B}=\int d\boldsymbol{B}. \tag{2}$$

For a unit dipole moment $\boldsymbol{m}$ in a magnetic field $\boldsymbol{B}$, the force that the magnetic dipole moment experiences can be derived by applying the Lorentz force law, and this is expressed in a vector form as(Griffith, 1989)

$$\boldsymbol{F}=(\boldsymbol{m}\cdot\nabla)\boldsymbol{B}. \tag{3}$$

When the pole face axis points to the surface of the air core solenoid, i.e., $m_x=m_y=0$, (3) can be simplified to

$$F_x=m_z\frac{\partial B_x}{\partial z}, \tag{4}$$

$$F_y=m_z\frac{\partial B_y}{\partial z}, \tag{5}$$

$$F_z=m_z\frac{\partial B_z}{\partial z}. \tag{6}$$

According to (4)~(6), we can discover that there are two types of forces present in an air core solenoid and permanent magnet system: radial force F_x, which is the same as F_y due to the symmetric geometry of the solenoid, and axial force, F_z. Their force characteristics are described in Fig. 2. The length of the solid lines indicates the magnitudes of each force. The symbol ⊙ and ⊗ denote that the current flows toward out of paper and toward in the paper respectively. When the upward-dipole-moment magnet is placed above the solenoid, F_x is zero at the z axis,

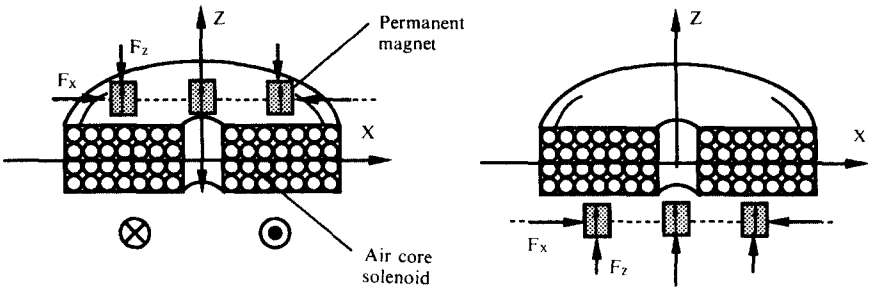

(a) Outside the air core

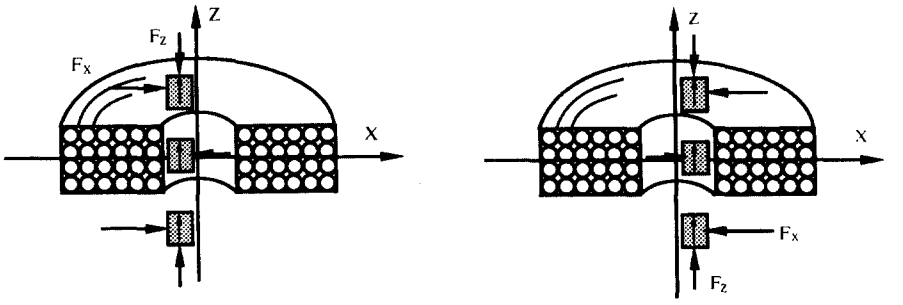

(b) Inside the air core

Fig. 2 Forec characteristics in a solenoid/magnet system

increases to some constant value in the middle, and decreases to zero at the edge of the solenoid. F_x has the same force characteristic when the magnet is placed below the solenoid. The force is directed toward to the core. In another word, the magnet experiences a pulling force toward the core when the magnet moves above and below the solenoid. When the magnet is placed inside the core, the radial force is also zero at the z axis, and it increases as the magnet approaches the core inner wall. However, the force is directed in an opposite direction. In another word, the magnet experiences a pushing force toward the inner wall.

F_z is zero at the center, and it is maximum a little away from the surface of the solenoid and then decreases steeply as the magnet moves away. F_z is a function of both the supplied current and displacement.

One thing to note from Fig. 2 is that a positive spring force is generated inside the air core along the z direction and negative spring force is generated outside the air core along the z direction. This fact reveals that the manipulator inside the air core can be stabilized in open loop due to the antagonistic property or push-and-push mechanism. For example, in case when the magnet is inside core as shown in Fig. 3(a), the manipulator is returning to an quilibrium point in the z-direction, where the manipulator weight, $m_a g$ balances to a recovery force, F_z. The z position of the manipulator is controlled by changing the input current. In case when the magnet is outside the core as shown in Fig. 3(b), the manipulator is returning to a certain equilibrium point by using another magnet and solenoid in pair in the opposite direction.

One more thing to be considered on employing the antagonistic structure is that the radial force is also generated together with the axial force. In Fig. 3 the radial force also exists besides the axial force. The radial force should be kept as small as possible because it works as a destabilizing force in some cases. This fact is reflected in designing the micro positioning system.

3. Design of Maglev Micro Positioning System

3.1 Preliminary design

Employing the antagonistic property obtained by using the air core solenoid and magnet in pair, we introduce a maglev micro positioning manipulator shaped as shown in Fig. 4. The box shaped manipulator consists of the top and bottom plates which are 10 cm × 10 cm flat squares and four connecting bars and two side bars which are 7 cm lengths and 1 cm widths. Fourteen magnets are mounted on the manipulator while fourteen coils paired with the magnets are fixed on the base frame. Light weight and rigidity are the two goals of the manipulator design to reduce an amount of current and manipulator structure deformation.

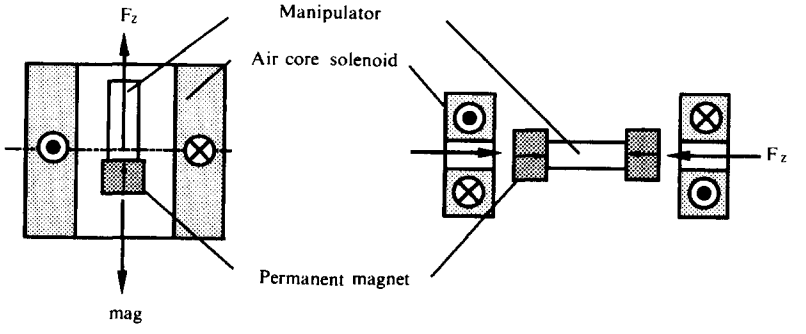

(a) When the magnet is inside the air core

(b) When the magnet is outside the air core

Fig. 3 Antagonistic structure produced by using a solenoid and permanent magnet in pair

Aluminum is used for the material because of its light weight. Several portions of the manipulator are taken away to reduce the weight. The net weight of the manipulator with the magnets is estimated to be about 220 grams.

Let's assume that the xyz coordinate system is fixed in the center of the manipulator and the XYZ coordinate system is fixed in the center of the base frame. We describe an arbitrary orientation of the manipulator in terms of Eulerian angles θ, ϕ and ψ as shown in Fig. 4.

The stability problems in the direction of X and Y are solved by using the two coils/magnets mounted on top and bottom in each connecting bars. Each pair is located at A, B, C, D, A', B', C', and D'. They are named as centering coils/magnets for convenience. The manipulator is stable because the recovery forces are increased as X or Y increases due to the antagonistic structure.

Also using the four coils/magnets in pairs located in the middle of the two plates, the stability problems in the direction of Z, ϕ and ψ are solved. Each pair is located at G, H, I and J, and they are named as levitating coils/magnets for convenience. The levitating magnets are placed as close to the edges as possible for better stability. The manipulator tends to recover against the ψ directed movement, for instance, because the axial force inside the core has the antagonistic property. The same phenomena happen in the direction of ϕ and Z.

On the other hand, it is unstable in the θ direction because a slight difference of the centering force generates a rotating torque. Further, the radial force inside the levitating coil helps rotate in the θ direction. Therefore, another pair of coil/magnet needs to be used to control θ direction. To this end, two pairs of coils/magnets which are diagonally mounted at E and F are used, and they are named as stabilizing coils/magnets for convenience. Attractive or repulsive force is generated depending on the magnitude of θ variation which can be obtained by measuring two points along the side of the manipulator. Therefore, from the above statement, it can be said that the proposed maglev system is internally stable in all directions except the θ direction.

We summarize the previous discussion in Fig. 4 as followings. The manipulator is driven to the desired X, Y, ϕ and ψ positions by adjusting the amount of the currents to the centering coils. The desired position in the Z direction is controlled by using the levitating coils. The inevitable instability in the θ direction is controlled by the stabilizing coils.

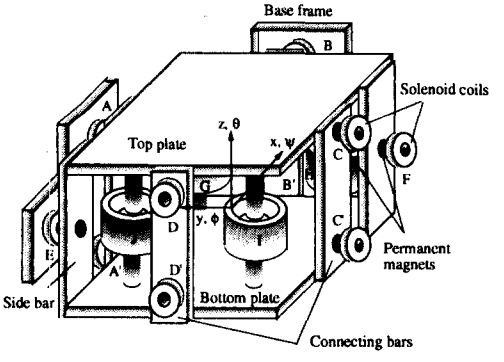

A,B,C,D,A',B',C', and D': centering coils/magnets
E and F: stabilizing coils/magnets
G,H,I, and J: levitating coils/magnets

Fig. 4 View of the 6 degree-of-freedom maglev micro positioning manipulator

3.2 Detailed design by force analysis

Several decisions regarding the dimensions of the solenoids and permanent magnets should be made to complete the maglev micro positioning system design. The magnet material is chosen to be advanced neodymium-iron-boron(NdFeB) rare earth magnet mainly for its high residual induction, 11,500 *Gauss*, which enhances the magnetic forces, and strong coercive force, 10,900 *Oersteds*, which lowers demagnetizing effect.

Let's investigate analytically how the solenoid and magnet dimensions affect the axial force. We use (6) with an explicit expression for the magnetic field density for an air core solenoid in the axial direction as given by Wangsness (Wangsness, 1979):

$$B_z=\frac{\mu_o Ni}{2l(D-d)}\left[(l+2z)\ln\left(\frac{D+\sqrt{D^2+(l+2z)^2}}{d+\sqrt{d^2+(l+2z)^2}}\right)\right]$$

$$+\frac{\mu_o Ni}{2l(D-d)}\left[(l-2z)\ln\left(\frac{D+\sqrt{D^2+(l+2z)^2}}{d+\sqrt{d^2+(l+2z)^2}}\right)\right], \quad (7)$$

where D, d, l and z are the solenoid outer diameter, inner diameter, length, and distance of the permanent magnet relative to the solenoid center. N and i are the number of coil turns and flowing current respectively. For the permanent magnet, a cylindrically shaped magnet is considered. D_m and l_m denote the diameter and length of the magnet respectively.

First, we examine the effect of the solenoid size on the axial force with the magnet size fixed. To make a fair comparison, we assume that the volume of the solenoid is constant, i.e., the wire diameter and the number of coil turns are constant. Figure 5 shows the effect of D, d and l on the force when z is fixed to $0.5l$, $0.7l$, $0.9l$, and $1.1l$ for $m_z=0.0309\ A/m$, $N=800$, and $i=1A$ (Note that $z=0.5l$ on the axis corresponds to the top of the solenoid). From this figure, we can get the following information:

(1) As D increases(or l decreases), the axial force, F_z increases for all z.

(2) As d decreases, F_z increases for all z. However, for a large absolute value of z(or as the magnet gets farther from the top surface of the solenoid), F_z increases only slightly as d decreases.

(3) An increase in D(or decrease in l) influences F_z more than an increase in d does. This tendency is less profound as the absolute value of z gets larger. In other words, D and l are more sensitive design parameters than d.

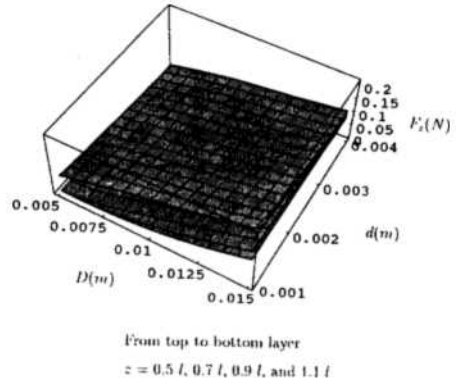

Fig. 5 Effect of the solenoid outer diameter, D and inner diameter, d on the axial force F_z

As a rule of thumb, a solenoid that is wider in outer diameter and shorter in length gives higher axial force than one with a smaller outer diameter and longer length when the volume of the solenoid is kept constant. The above design criteria are reflected as setting the centering magnet diameter, D_m and inner diameter of the centering coil, d to 4 mm and 8 mm respectively.

Next, we examine the effect of the magnet size on the axial force. If we approximate a magnet as a stack of thin magnet layers, we can add the contributions of each of the magnet layers to get the total magnetic flux. We start this investigation for the centering coil with the solenoid size fixed as $D=18$ mm, $d=8$ mm, $l=10$ mm, $N=1000$ and with $1A$ current. Figure 6(a) shows the force curves plotted from data taken along the z axis with l_m equal to 1, 2, 3, 4, 5, and 6 mm, and with D_m equal to 4 mm. We discover that the axial force increases with increasing l_m; however, the increasing rate is slightly decreased. Similar results are obtained with different solenoid sizes. The length of the centering magnet, l_m is chosen as 4 mm with the consideration of efficiency of the axial force production per magnet mass. The air gap between the coil and magnet should be maintained so that a high and linear spring constant can be obtained, and this is chosen referring to Fig. 6(a) as about 2 mm. Figure 6(b) shows the force curves for different currents with the determined dimensions.

We continue this investigation for the levitating coil, with the solenoid size fixed as $D=30$ mm, $d=15$ mm, $l=40$ mm, $N=1000$ and $1A$ current. Figure 7(a) shows the force curves for the levitating coil plotted from data taken along the z axis with l_m equal to 2, 4, 6, 8, and 10 mm, and with D_m equal to 10 mm. In a similar way, l_m is chosen as 10 mm with the consideration of sufficient force to overcome the manipulator gravitational weight, $m_a g$ as well as the force efficiency per magnet mass. The levitating magnet should be placed where maximum force occurs. The levitating position is chosen to be -15 mm referring to

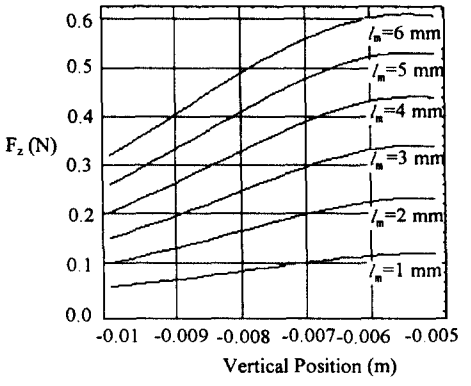

Fig. 6 (a) Centering force curves for different magnet lengths

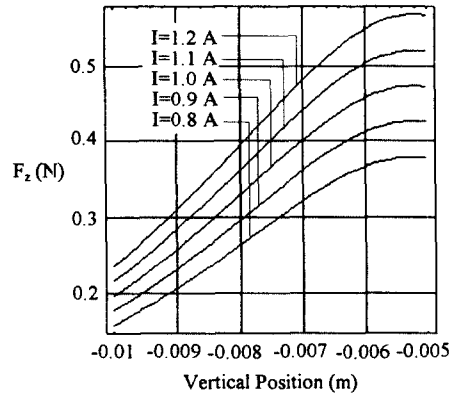

Fig. 6 (b) Centering force corves for different currents

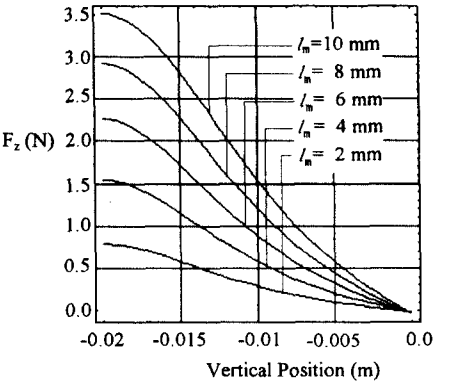

Fig. 7 (a) Levitating force curves for different magnet lengths

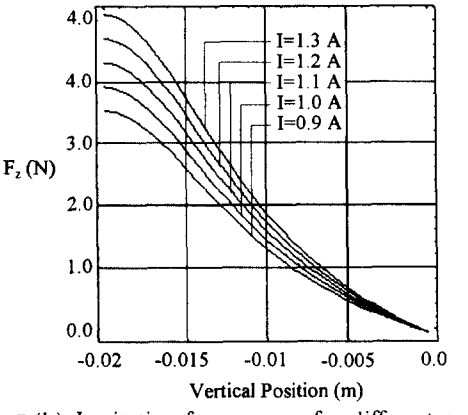

Fig. 7 (b) Levitating force curves for different currents

Fig. 7(a). Considering that a small air gap between the magnets and core reflects a higher levitating force, the -15 mm inner diameter of levitating coil enables the manipulator to have 1 or 2 mm translational movement inside core. Figure 7(b) shows the force curves for different currents with the determined dimensions.

In the centering magnets and levitating magnets, the radial forces work as destabilizing forces. For the determined levitating coil and magnet dimensions, the radial forces inside the air core are investigated by using (1) to (4). The radial forces for different z locations are shown in Fig. 8. Similarly, for the determined centering coil and magnet dimensions, the radial forces outside the air core can be investigated.

The wires of the levitating coil and centering coil are chosen to be 25 *AWG*(American wire gauge): its 0.5 mm diameter simplifies the work of defining coil coordinate for calculating the forces and its moderate mechanical flexibility reduces the coil winding effort. The dimensions of the stabilizing coils/magnets are chosen as the same as the dimensions of centering coils/mag-

Table 1 Design summary of centering coil/magnet

Parameter	Description	Value
D	Solenoid outer diameter	18 mm
d	Solenoid inner diameter	8 mm
l	Solenoid length	10 mm
N	Number of wires on each side	40×25
D_m	Magnet diameter	4 mm
l_m	Magnet length	4 mm

Table 2 Design summary of levitating coil/magnet

Parameter	Description	Value
D	Solenoid outer diameter	30 mm
d	Solenoid inner diameter	15 mm
l	Solenoid length	40 mm
N	Number of wires on each side	12×80
D_m	Magnet diameter	10 mm
l_m	Magnet length	8 mm

nets to simplify the dynamic modeling. Table 1 to 2 summarize the design parameters.

4. Modeling of System Dynamics

To understand the dynamics of the maglev positioning system, we describe an arbitrary orientation of the manipulator in terms of Eulerian angles. The equations of motion for the manipulator rotation in terms of Eulerian angles can be derived by employing Lagrange's equations. By

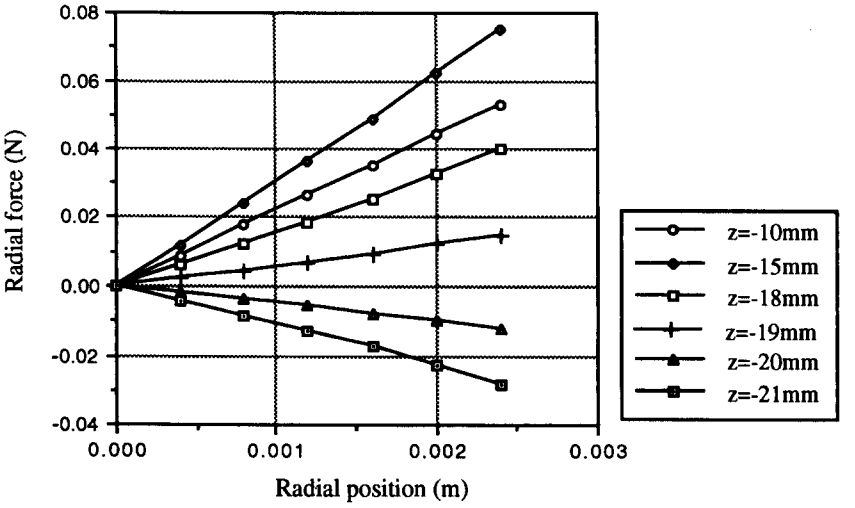

(a) For different z locations

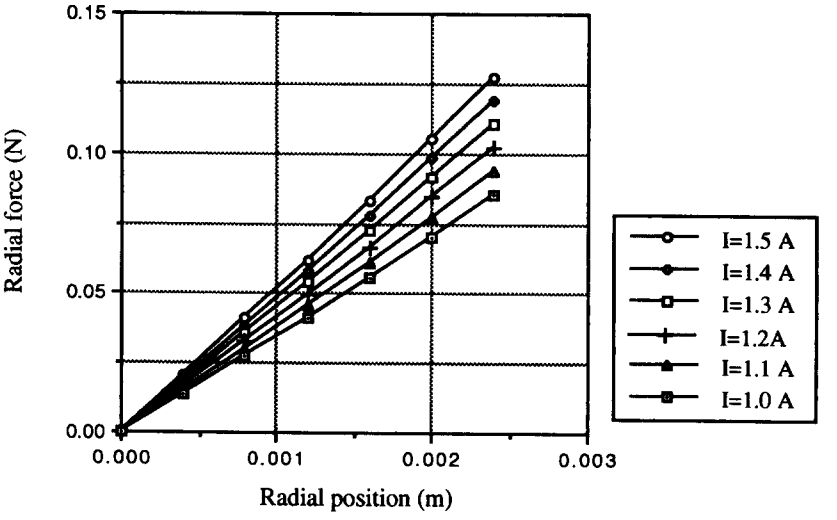

(b) For different currents

Fig. 8 Radial force curves inside the air core

letting the xyz coordinate system be coincident with the principal axes, the rotational kinetic energy can be expressed as

$$T_{rot}=\frac{1}{2}(I_x\omega_x^2+I_y\omega_y^2+I_z\omega_z^2) \tag{8}$$

where ω_x, ω_y, and ω_z are the angular velocities with respect to the x, y, and z axis respectively. In order to use Lagrange's equation, ω_x, ω_y, and ω_z are required to be expressed in terms of Eulerian angles. Their relations are(Greenwood, 1965)

$$\omega_x=\dot{\psi}-\dot{\theta}\sin\phi, \tag{9}$$
$$\omega_y=\dot{\phi}\cos\psi+\dot{\theta}\cos\phi\sin\psi, \tag{10}$$
$$\omega_z=\dot{\theta}\cos\phi\cos\psi-\dot{\phi}\sin\psi. \tag{11}$$

Substituting these relations into (8) and using Lagrange's equations, we obtain a set of complicated equations of motion in terms of Eulerian angles. With an assumption of small angle rotation, which is valid particularly for our application, we can simplify the equations of motion by letting $\sin\theta=0$, $\cos\theta=1$, and all the second or higher order terms equal zero, resulting in very simple equations of motion,

$$I_z\ddot{\theta}=M_\theta, \tag{12}$$
$$I_y\ddot{\phi}=M_\phi, \tag{13}$$
$$I_x\ddot{\psi}=M_\psi. \tag{14}$$

In these equations, M_θ, M_ϕ, and M_ψ are external moments in terms of Eulerian angles, and I_x, I_y, and I_z are the principal moments of inertia. Since we are going to use these equations to calculate external forces and torques in XYZ coordinate system, a transformation from M_θ, M_ϕ and M_ψ to T_X, T_Y, and T_Z is necessary. Using the rotational sequences of Eulerian angles defined previously, the relations between them can be simplified, with the same small angle assumption, as

$$M_\theta=T_Z, \tag{15}$$
$$M_\phi=T_Y-T_X\theta, \tag{16}$$
$$M_\psi=T_X+T_Y\theta-T_Z\phi. \tag{17}$$

Performing variational calculus on these equations with respect to the origin, $\phi=\theta=0$ and using from (12) to (14), we obtain

$$I_z\delta\ddot{\theta}=\delta T_Z, \tag{18}$$
$$I_y\delta\ddot{\phi}=\delta T_Y, \tag{19}$$
$$I_x\delta\ddot{\psi}=\delta T_X, \tag{20}$$

since $T_X \mid_{\phi=0,\theta=0}=T_Y \mid_{\phi=0,\theta=0}=T_Z \mid_{\phi=0,\theta=0}=0$.

F_X, F_Y, and F_Z that are responsible for the translational motions can be obtained from the direct summation of forces. After taking the first variations, they can be expressed as

$$m_a\delta\ddot{x}=\delta F_X, \tag{21}$$
$$m_a\delta\ddot{y}=\delta F_Y, \tag{22}$$
$$m_a\delta\ddot{z}=\delta F_Z. \tag{23}$$

To obtain expressions for T_X, T_Y, T_Z, F_X, F_Y, and F_Z, all forces acting on the manipulator are shown in Fig. 9, where the first subscripts of F denote the magnet locations on which forces are acting, and the second subscripts of F denote the directions to which forces are acting.

First, the positions of the magnets with respect to the XYZ coordinates must be investigated. The XYZ coordinates of points fixed in the xyz system after θ, ϕ, ψ rotation can be obtained by

$$\begin{bmatrix}X\\Y\\Z\end{bmatrix}=\boldsymbol{T}^T\begin{bmatrix}x\\y\\z\end{bmatrix}, \tag{24}$$

where

$$\boldsymbol{T}^T=\begin{bmatrix}\cos\theta\cos\phi & \cos\theta\sin\phi\sin\psi-\sin\theta\cos\psi & \cos\theta\sin\phi\cos\psi+\sin\theta\sin\psi\\ \sin\theta\cos\phi & \sin\theta\sin\phi\sin\psi+\cos\theta\cos\psi & \sin\theta\sin\phi\cos\psi-\cos\theta\sin\psi\\ -\sin\phi & \cos\phi\cos\psi & \cos\phi\cos\psi\end{bmatrix}. \tag{25}$$

Employing the displacement expressions of each magnet, the forces in Fig. 9 can be expressed in terms of the generalized coordinates. Each force is modeled as a spring force which is a function of displacement and current:

$$F_{AX}=K_{AX}(-a\theta+e\phi+X)+K_{AXi}I_A,$$
$$F_{AY}=K_{AY}(Y-e\psi)+K_{AYi}I_A,$$
$$F_{AZ}=K_{AZ}(a\psi+Z)+K_{AZi}I_A, \tag{26}$$
$$F_{BX}=K_{BX}(X+e\phi)+K_{BXi}I_B,$$
$$F_{BY}=K_{BY}(a\theta-e\psi+Y)+K_{BYi}I_B,$$
$$F_{BZ}=K_{BZ}(-a\phi+Z)+K_{BZi}I_B, \tag{27}$$
$$F_{CX}=K_{CX}(a\theta+e\phi+X)+K_{CXi}I_C,$$
$$F_{CY}=-K_{CY}(Y-e\psi)+K_{CYi}I_C,$$
$$F_{CZ}=K_{CZ}(-a\psi+Z)+K_{CZi}I_C, \tag{28}$$

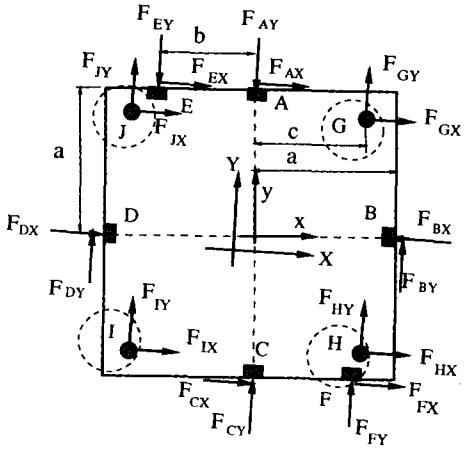

(a) Top view

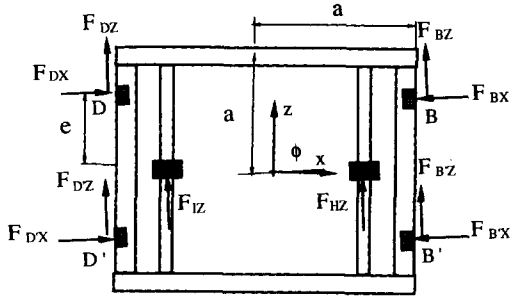

(b) Side view

Fig. 9 Forces acting on the manipulator

$$
\begin{aligned}
F_{DX} &= -K_{DX}(X+e\phi)+K_{DXi}I_D,\\
F_{DY} &= K_{DY}(-a\theta-e\phi+Y)+K_{DYi}I_D\\
F_{DZ} &= K_{DZ}(a\phi+Z)+K_{DZi}I_D, \qquad (29)\\
F_{EX} &= K_{EX}(-a\theta+X)+K_{EXi}I_E,\\
F_{EY} &= K_{EY}(Y-b\theta)+K_{EYi}I_E,\\
F_{EZ} &= K_{EZ}(b\phi+a\psi+Z)+K_{EZi}I_E, \qquad (30)\\
F_{FX} &= K_{FX}(a\theta+X)+K_{FXi}I_F,\\
F_{FY} &= -K_{FY}(Y+b\theta)+K_{FYi}I_F,\\
F_{FZ} &= K_{FZ}(-b\phi-a\psi+Z)+K_{FZi}I_F, \qquad (31)\\
F_{GX} &= K_{GX}(X-c\theta)+K_{GXi}I_G,\\
F_{GY} &= K_{GY}(Y+c\theta)+K_{GYi}I_G,\\
F_{GZ} &= -K_{GZ}(Z-c\phi+c\psi)+K_{GZi}I_G, \qquad (32)\\
F_{HX} &= K_{HX}(X+c\theta)+K_{HXi}I_H,\\
F_{HY} &= K_{HY}(Y+c\theta)+K_{HYi}I_H,\\
F_{HZ} &= -K_{HZ}(Z-c\phi-c\psi)+K_{HZi}I_H, \qquad (33)\\
F_{IX} &= K_{IX}(X+c\theta)+K_{IXi}I_I,\\
F_{IY} &= K_{IY}(Y-c\theta)+K_{IYi}I_I,\\
F_{IZ} &= -K_{IZ}(Z+c\phi-c\psi)+K_{IZi}I_I, \qquad (34)\\
F_{JX} &= K_{JX}(X-c\theta)+K_{JXi}I_J,\\
F_{JY} &= K_{JY}(Y-c\theta)+K_{JYi}I_J,\\
F_{JZ} &= -K_{JZ}(Z+c\phi+c\psi)+K_{JZi}I_J, \qquad (35)
\end{aligned}
$$

where a, b, c and e are the distances defined in Fig. 9. K_{AX}, K_{AY} and K_{AZ} denote spring constants which relate the forces acting on the magnet A with respect to the X, Y and Z direction of the solenoid A respectively. K_{AXi}, K_{AYi} and K_{AZi} denote force constants which relate the forces acting on the magnet A with respect to the current which flows in the solenoid A. Similar definitions are applied to the rest of the constants. Then, the spring constants and force constants have the following values:

$$
\begin{aligned}
K_{AX} &= K_{AZ}=\frac{\partial F_{AX}}{\partial X}\Big|_{I=I_{co},X=0}=K_{cr},\\
K_{AY} &= \frac{\partial F_{ZY}}{\partial Y}\Big|_{I=I_{co},Y=a}=K_{ca}, \qquad (36)\\
K_{AXi} &= K_{AZi}=\frac{\partial F_{AX}}{\partial I}\Big|_{I=I_{co},X=0}=0,\\
K_{AYi} &= \frac{\partial F_{AY}}{\partial I}\Big|_{I=I_{co},Y=a}=K_{cai}, \qquad (37)
\end{aligned}
$$

where I_{co} is the rated current in the centering coil and it is $1A$. The same dimensions of the rest of the centering coils/magnets lead to the following results:

$$
\begin{aligned}
&K_{BX}=K_{ca},\ K_{BY}=K_{BZ}=K_{cr},\\
&K_{BXi}=K_{cai},\ K_{BYi}=K_{BZi}=0, \qquad (38)\\
&K_{CX}=K_{CZ}=K_{cr},\ K_{CY}=K_{ca},\\
&K_{CXi}=K_{CZi}=0,\ K_{CYi}=K_{cai}, \qquad (39)\\
&K_{DX}=K_{ca},\ K_{DY}=K_{DZ}=K_{cr},\\
&K_{DXi}=K_{cai},\ K_{DYi}=K_{DZi}=0. \qquad (40)
\end{aligned}
$$

Regarding to the stabilizing coils/magnets and the levitating coils/magnets, without being redundant, the spring constants and force constants are

$$
\begin{aligned}
&K_{EX}=K_{EZ}=K_{EY}=0,\\
&K_{EXi}=K_{EYi}=0,\ K_{EYi}=K_{sai}, \qquad (41)\\
&K_{FX}=K_{FZ}=K_{FY}=0,\\
&K_{FXi}=K_{FZi}=0,\ K_{FYi}=K_{sai}, \qquad (42)\\
&K_{GX}=K_{GY}=K_{lr},\ K_{GZ}=K_{la},\\
&K_{GXi}=K_{GYi}=0,\ K_{GZi}=K_{lai}, \qquad (43)\\
&K_{HX}=K_{IX}=K_{JX}=K_{HY}\\
&\quad =K_{IY}=K_{JY}=K_{lr}, \qquad (44)\\
&K_{HZ}=K_{IZ}=K_{JZ}=K_{la}, \qquad (45)\\
&K_{HXi}=K_{IXi}=K_{JXi}=K_{HYi}\\
&\quad =K_{IYi}=K_{JYi}=0, \qquad (46)
\end{aligned}
$$

$$K_{HZi}=K_{IZi}=K_{JZi}=K_{lai}. \tag{47}$$

All the spring constants K_{ca}, K_{cr}, K_{la}, K_{lr} and the force constants K_{cai}, K_{sai} and K_{lai} are calculated from the analytical results shown in Fig. 6 through Fig. 8. We have $K_{sai}=K_{cai}$ because the dimensions of the stabilizing coils/magnets are chosen as the same as the dimensions of centering coils/magnets. The specifications of the manipulator and the system parameters are listed in Table 3. The rated current and Z location in the levitating coil are $0.9A$ and -15 mm. Similar procedures can be taken for the forces acting on the magnets A', B', C' and D'.

δF_X, δF_Y and δF_Z are expressed from direct summation of the first variation of each force. Employing the displacement expressions of each magnet, δT_X, δT_Y and δT_Z can be expressed with respect to the point where all variables are zero. Neglecting the second order or higher orders terms due to the same small angle assumption, and using from (18) and (23), a complete analytical model can be derived as follows:

$$\begin{aligned} &m_a\delta\ddot{X}+4(K_{ca}-K_{lr}-K_{cr})\delta X \\ &=K_{cai}(-\delta I_B-\delta I'_B+\delta I_D+\delta I'_D), \end{aligned} \tag{48}$$

$$\begin{aligned} &m_a\delta\ddot{Y}+4(K_{ca}-K_{lr}-K_{cr})\delta \\ &=K_{cai}(-\delta I_A-\delta I'_A+\delta I_C+\delta I'_C) \\ &\quad+K_{sai}(-\delta I_E+\delta I_F), \end{aligned} \tag{49}$$

$$\begin{aligned} &m_a\delta\ddot{Z}+4(K_{la}-2K_{cr})\delta Z \\ &=K_{lai}(\delta I_G+\delta I_H+\delta I_I+\delta I_J), \end{aligned} \tag{50}$$

$$\begin{aligned} &I_x\delta\ddot{\psi}+4(e^2K_{ca}+c^2K_{la}-(a^2+e^2)K_{cr})\delta\psi \\ &=eK_{cai}(\delta I_A-\delta I'_A-\delta I_C+\delta I'_C) \\ &\quad+cK_{lai}(\delta I_G-\delta I_H-\delta I_I+\delta I_J), \end{aligned} \tag{51}$$

$$\begin{aligned} &I_y\delta\ddot{\phi}+4(e^2K_{ca}+c^2K_{la}-(a^2+e^2)K_{cr})\delta\phi \\ &=eK_{cai}(-\delta I_B+\delta I'_B+\delta I_D-\delta I'_D) \\ &\quad+cK_{lai}(-\delta I_G-\delta I_H+\delta I_I+\delta I_J), \end{aligned} \tag{52}$$

$$\begin{aligned} &I_z\delta\ddot{\theta}-8(a^2K_{cr}+c^2K_{lr})\delta\theta \\ &=bK_{sai}(\delta I_E+\delta I_F). \end{aligned} \tag{53}$$

Substituting the numerical values of the spring constants and force constants, dropping δ sign in

Table 3 The specifications of the manipulator and the system parameters

Parameter	Description	Value
a	Distance from the center to the edges of the manipulator in the x direction	50 mm
b	Distance from the center to the stabilizing magnets	41 mm
c	Distance from the center to the levitating magnets	28 mm
e	Distance from the center to the centering magnets to the z direction	25 mm
m_a	Manipulator mass	220 grams
I_x	Principal moment of inertia about the x axis	3.25 kg·cm^2
I_y	Principal moment of inertia about the y axis	3.31 kg·cm^2
I_z	Principal moment of inertia about the z axis	3.24 kg·cm^2
K_{ca}	Spring const. of the axial force in the centering coil/magnet(C/M)	32.9 N/m
K_{la}	Spring const. of the axial force in the levitating C/M	57.1 N/m
K_{cr}	Spring const. of the radial force in the centering C/M	10.2 N/m
K_{lr}	Spring const. of the radial force in the levitating C/M	16.5 N/m
K_{cal}	Force const. of the axial force in the centering C/M	0.14 N/A
K_{sal}	Force const. of the axial force in the stabilizing C/M	0.14 N/A
K_{lal}	Force const. of the axial force in the levitating C/M	0.79 N/A

from (48) to (53) and assuming $I_A=I'_A$, $I_B=I'_B$, $I_C=I'_C$, and $I_D=I'_D$ for simplicity, we obtain the linearized equations of motion as

$$\ddot{X}+118.2X=0.28(-I_B+I_D), \quad (54)$$

$$\ddot{Y}+118.2Y = 0.28(-I_A+I_C)+0.14(-I_E+I_F), \quad (55)$$

$$\ddot{Z}+672.7Z=0.79(I_G+I_H+I_I+I_J), \quad (56)$$

$$\ddot{\psi}+400\psi=68.1(I_G-I_H-I_I+I_J), \quad (57)$$

$$\ddot{\phi}+392.7\phi=66.8(-I_G-I_H+I_I+I_J), \quad (58)$$

$$\ddot{\theta}-936.7\theta=17.7(I_E+I_F). \quad (59)$$

From the above equations of motion, we can observe that each motion is decoupled from the rest of the motions, and it is internally stable except for the θ. Therefore the only θ directed rotation needs to be stabilized. Theoretically, the stabilization controller for θ motion as well as the centering and levitating controller should be designed based on this model. One more thing to observe is that the big positive constants associated with the ψ, ϕ, and Z variables suggest that their motions are very stiff.

Additionally, each motion except the θ motion is anticipated to oscillate to its natural frequency. The proposed modeling process can be experimentally verified by the oscillation motions. Figure 10 shows the free vibration of Z and ψ(or ϕ) with the initial conditions. This result is obtained by controlling the only unstable modes, θ with PID controllers. From the figure, the natural frequency of around 5 Hz and 3.3 Hz are observed in the Z and ψ(or ϕ) modes respectively. Their natural frequencies from the analytical model, Eqs. (56) and (57), are 4.2 Hz and 3.1 Hz respectively. They are almost alike each other. The damping force in the actual system is likely due to the air damping and electromotive force generated when the manipulator is moving up and down. Using the logarithmic decrement method, the damping coefficients are estimated as 0.66 N·s/m and 0.00065 N·m·s for Z and ψ motion respectively.

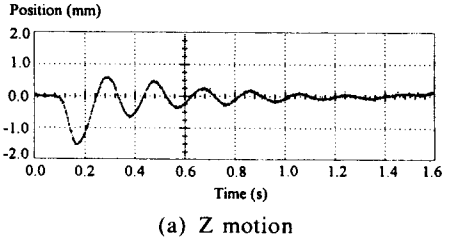

(a) Z motion

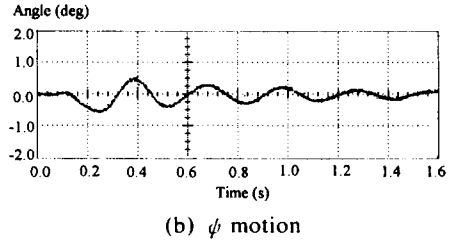

(b) ψ motion

Fig. 10 Free vibration of the manipulator

5. Conclusion

A 6 degree-of-freedom magnetically suspended frictionless system is designed and modeled. Push-and-push forces, i.e., antagonistic forces are employed by using the force characteristics of the air core solenoid/permanent magnet to increase the dynamic stability of the magnetic suspension system. To design the solenoid and the size of magnet, those effects on the axial force are investigated, and their sizes are determined after considering the produced maximum force and their efficiency of the axial force production per magnet mass.

From the dynamic equations of motion, it is verified that the proposed magnetic suspended system is internally stable in all directions except the θ direction. The proposed analytic model was experimentally verified by comparing the free vibration characteristics of the manipulator.

References

Fujita, H. and Omodaka, A., 1987, "Electrostatic Actuators for Micromechatronics," *IEEE Micro Robots and Teleoperators Workshop*, Hyannis, MA.

Greenwood, Donald T., 1965, *Principle of Dynamics*, Prentice-Hall, Englewood Cliffs, New jersey.

Griffith, David J., 1989, *Introduction to Electrodynamics*, 2nd ed., Prentice Hall, Englewood Cliffs, N.J.

Hayt, William H., 1989, *Engineering Electro-*

magnetics, McGraw Hill, New York.

Higuchi, T., Yamagata, Y., Furutani, K. and Kudoh, K., 1990, "Precise Positioning Mechanism Utilizing Rapid Deformations of Piezoelectric Elements," *IEEE Micro Electro Mechanical Systems*, Napa Valley, CA, Feb., 11 ~14.

Hollis, R. L., Allan, A. P. and Salcudean, S., 1987, "A Six Degree-of-Freedom Magnetically Levitated Variable Compliance Fine Motion Wrist," *4th Intn. Symp. on Robotics Res.*, Santa Cruz, CA.

Kuribayashi, K., 1989, "Micro Actuator Using Shape Memory Alloy for Micro Robot," *International Conf. on Advanced Mechatronics*, pp. 109 ~114.

Mehregany, M., Nagarkar, P., Senturia, S. and Lang, J., 1990, "Operation of Microfabricated Harmonic and Ordinary Side-Drive Motors," *IEEE Micro Electro Mechanical Systems*, Napa Valley, CA.

Ohnuki, H. and Fukui, Y., 1982, "Three-Dimensional Actuators for Optical Head," *SPIE Optical Disk Technology*, Vol. 329, pp. 103~108.

Sinha, P. K., 1987, *Electromagnetic Suspension: Dynamics and Control*, Peter Peregrins, London.

Smith, D. and Elrod, S., 1985, "Magnetically Driven Micropositioners," *Review of Scientific Instruments*, 56(10), pp. 1970~1971.

Trimmer, W. S. and Gabriel, K. J., 1987, "Design Considerations for Practical Electrostatic Micro Motor," *Sensors and Actuators*, pp. 189~206.

Tsuda, M., Higuchi, T. and Fujiwara, S., 1987, "Magnetic Supported Intelligence hand for Automated Precise Assembly," *Proc. of Conf. on Industrial Electronic, Control and Instrumentation*, SPIE Vol. 05, pp. 926~933.

Umetani, Y. and Suzuki, H., 1980, "Piezo-Electric Micro Manipulator in Multi-Degree of Freedom with Tactile Sensibility," *10th International Symposium on Industrial Robots*, pp. 571 ~579.

Wangsness, R. K., 1979, *Electromagnetic Fields*, John Wiley & Sons, New York.